C Journal of Carbon Research

MDPI

Article

Application of GUITAR on the Negative Electrode of the Vanadium Redox Flow Battery: Improved $V^{3+/2+}$ Heterogeneous Electron Transfer with Reduced Hydrogen Gassing

Humayun Kabir [1], Isaiah O. Gyan [2], Jeremy D. Foutch [1], Haoyu Zhu [1] and I. Francis Cheng [1,*]

[1] Department of Chemistry, University of Idaho, Renfrew Hall 116, 875 Perimeter Dr, MS 2343, Moscow, ID 83844, USA; kabi4669@vandals.uidaho.edu (H.K.); fout5025@vandals.uidaho.edu (J.D.F.); zhu1099@vandals.uidaho.edu (H.Z.)

[2] Intel Corporation, Ronler Acres, Hillsboro, OR 97124, USA; isaiah.o.gyan@intel.com

* Correspondence: ifcheng@uidaho.edu; Tel.: +1-208-885-6387

Academic Editor: Craig E. Banks

Received: 7 January 2016; Accepted: 7 April 2016; Published: 19 April 2016

Abstract: GUITAR (Graphene from the University of Idaho Thermolyzed Asphalt Reaction) has the classical basal and edge plane morphology of graphites and thin layer graphenes with similar X-ray photoelectron spectroscopy (XPS), Raman and IR characteristics. However previous investigations indicated GUITAR is different electrochemically from graphenes and classical graphites. GUITAR has faster heterogeneous electron transfer across its basal plane and an electrochemical window that exceeds graphitic materials by 1 V. These beneficial properties are examined for application in the negative electrode of the vanadium redox flow battery (VRFB). Graphitic materials in this application suffer from hydrogen gassing and slow electron transfer kinetics for the $V^{2+/3+}$ redox couple. Cyclic voltammetry of the $V^{2+/3+}$ redox couple (0.05 M V^{3+} in 1 M H_2SO_4) on bare KFD graphite felt gives an estimated standard rate constant (k^0) of 8.2×10^{-7} cm/s. The GUITAR-coated KFD graphite felt improves that quantity to 8.6×10^{-6} cm/s. The total contribution of the cyclic voltammetric currents at −1.0 V *vs.* Ag/AgCl to hydrogen evolution is 3% on GUITAR-coated KFD graphite felt. On bare KFD graphite felt, this is 22%. These results establish GUITAR as an excellent alternative material for the negative electrode in the vanadium redox flow battery.

Keywords: GUITAR; KFD graphite felt; vanadium redox flow battery; hydrogen evolution; heterogeneous electron transfer rate; cathodic limit

1. Introduction

GUITAR (Graphene from the University of Idaho Thermolyzed Asphalt Reaction) is a hypothesized new allotrope of carbon that offers many advantages over other conventional carbon-based materials in electrochemical applications [1,2]. When compared to graphite, graphene and other planar lamellar carbon materials, GUITAR possesses significantly faster electron transfer kinetics on the basal plane (BP), which serves as the most practical electrode surface in most applications [1]. Electron transfer at the surface of graphite is seen to be more favored at the terminating edges and grain boundaries as compared to the basal plane. This behavior is not observed with GUITAR. In previous work, we demonstrate that the kinetics of both the edges as well as the planar surfaces of GUITAR are equally fast in $Fe(CN)_6^{4-/3-}$, which is one of several properties which gives GUITAR a significant advantage over other carbon electrode materials in electrochemical applications [1]. The facile heterogeneous electron transfer (HET) rate of Basal Plane-GUITAR (BP-GUITAR) is attributed to increased density of electronic states (DOS) from the structural defects

within its molecular planes [1]. Also of great interest is GUITAR's large potential window for operation [1]. On the cathodic side, GUITAR's overpotential for hydrogen evolution exceeds other graphitic materials [1]. On the anodic side, GUITAR exhibits high resistance to corrosion and oxygen gassing. Taken together, GUITAR has a 3 V aqueous electrochemical window at 200 $\mu A/cm^2$, which is similar to boron doped diamond electrodes and exceeds other graphitic materials by 1 volt [2–5]. These properties make GUITAR ideally suited for applications in batteries, fuel cells, ultracapacitors, water purification, solar energy conversion devices, and electrochemical sensors [2].

Redox flow batteries (RFB) offer economical advantages and will find applications in grid-level power buffering [6–8]. RFBs are also free from the constraints of cycle-life limitations and are ideally suited for electrical energy storage applications including frequency regulation, load following, peak shaving and energy time shift [6,8,9]. The all-vanadium redox flow battery (VRFB) is a promising RFB and is based on the reactions of $V^{3+/2+}$ and $V^{4+/5+}$ [10]. VRFB's possess high efficiency operation as evidenced by fast response rates, deep discharge levels, long life and high discharge rates, while maintaining very low self-discharge rates. One particular advantage over several other redox flow batteries is that the cross mixing of anolytes and catholytes will not result in severe catastrophic reactions, as both contain vanadium ions [10–13].

To increase power and energy densities, all flow batteries require both fast HET rates as well as minimized parasitic electrode reactions. In the negative cell of VRFB, two major issues are of concern: (i) slow HET rates with the $V^{3+/2+}$ redox couple and (ii) parasitic hydrogen evolution [14–16]. A consequence of the former is low power density and low energy efficiency whereas the latter results in a loss in both coulombic and energy efficiency of the battery [17]. Parasitic evolution of hydrogen gas can interrupt the electrolyte flow, lead to changes in the pH, increase the cell resistance and finally dissipate the total energy [11,17,18]. Formation of hydrogen gas bubbles on negative electrode also blocks the electrode surface for $V^{3+/2+}$ HET [14]. Approximately 5%–25% of charging current is lost due to the parasitic hydrogen evolution at negative half of the VRBs. These hydrogen evolution percentages are calculated based on the given values/graphs in literature [17–21]. Therefore, minimization of parasitic hydrogen evolution in negative cells is critical for a durable and economically viable VRB. It is notable that GUITAR has a hydrogen overpotential of 900 mV *vs.* SHE in 1 M H_2SO_4 which exceeds graphite by over 300–500 mV [22].

In order to increase $V^{3+/2+}$ HET rates, the electrode material should have a high surface area but also be mechanically and chemically stable [20,23,24]. Active research is going on to identify such materials with the greatest focus being on carbon and graphite felts [25–28]. These electrodes offer cost effectiveness but suffer from slow $V^{3+/2+}$ HET rates and from significant parasitic hydrogen evolution [17,29]. In previous investigations GUITAR exhibited facile HET rates with $Fe(CN)_6^{3-/4-}$ and $Ru(NH_3)_6^{2+/3+}$ redox couples [22,30]. In this investigation, we assess the HET rate constant for $V^{3+/2+}$ redox system and contribution of hydrogen evolution on the overall voltammetric current on GUITAR flake, KFD graphite felt and GUITAR coated KFD graphite felt electrodes.

2. Results and Discussion

2.1. GUITAR Coated Graphite Felt Electrode

Electrode materials used in the VRFB are often carbon and graphite felts, which have relatively high surface area and allow for electrolyte flow through the fibers [20,31–33]. In this investigation, KFD graphite felt (Figure 1A) was examined as an electrode material for VRFBs. Figure 1C shows the GUITAR-coated KFD graphite felt material (GUITAR/KFD), which has the metallic luster seen in previous studies using flat electrode configurations. Figure 1B is a photograph of graphite exposed to the same temperatures as the TAR but without roofing tar precursors, which shows noticeable contraction. In order to determine the depth of deposition, scanning electron microscopy (SEM) was conducted on as-received and GUITAR-coated KFD graphite felt (Figure 2). Fiber thickness of the bare felt measured in this work is within literature range and is measured as 8.70 ± 0.46 μm ($n = 10$) [34].

Deposition of GUITAR results in an increase in fiber thickness to 12.34 ± 0.34 μm (n = 10) indicating an estimated depth of the deposited GUITAR layer of 1.8 μm. Also notable is that deposition of GUITAR apparently fills pores and smoothens the graphite felt fibers (Figure 2). The "smooth" (or true) surface areas of the KFD graphite felt and GUITAR/KFD were calculated assuming the felt electrode is made up of cylindrical graphite fibers as considered in Smith *et al.* [35] (more detail in supporting information, Table S1). The "smooth" surface area is found to be 64.4 cm^2 per cm^2 geometric area for KFD graphite felt and 61.6 cm^2 per cm^2 geometric area for GUITAR- coated KFD graphite felt. The electrochemical surface area (ECSA) of the KFD graphite felt and GUITAR/KFD felt electrodes were estimated from the Randles–Sevcik equation [36] using cyclic voltammograms on the electrodes in 1 mM $Fe(CN)_6^{3-/4-}$ (see Table S2). The electrochemical surface area (ECSA) of the KFD graphite felt was obtained as 61.5 cm^2 per cm^2 geometric area which is consistent with theoretical value. However, for GUITAR/KFD felt, the ECSA is 50.6 cm^2 per cm^2 geometric area which is around 15% less than the true surface area.

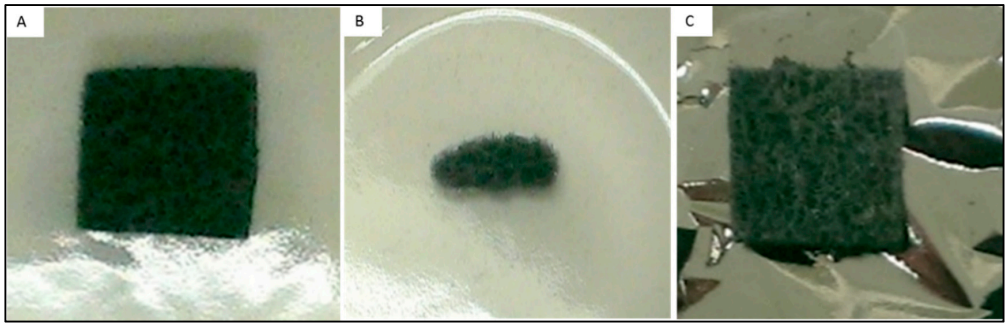

Figure 1. Photograph of (**A**) untreated graphite felt (geometric area 1 cm^2) (**B**) the same material heated for 25 min in the absence of GUITAR starting material and (**C**) GUITAR-coated graphite felt (geometric area 1 cm^2).

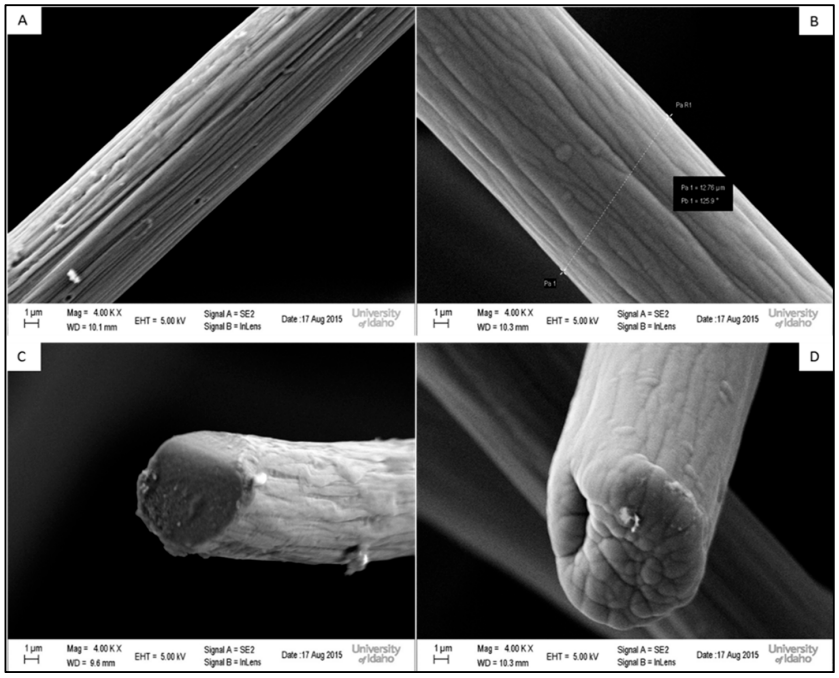

Figure 2. Scanning electron micrographs of as-obtained graphite felt (**A**,**C**) and GUITAR-coated graphite felt (**B**,**D**). Average thicknesses for as-obtained graphite felt (**A**,**C**) is obtained as 8.70 ± 0.46 μm (n = 10) and for GUITAR-coated graphite felt (**B**,**D**) is 12.34 ± 0.34 μm (n = 10).

2.2. Estimation of Hydrogen Overpotential by Cyclic Voltammetry in 1 M H_2SO_4

Cathodic limits at 200 μA/cm^2 in 1 M H_2SO_4 for graphitic materials lie between −0.3 V to −0.5 V (*vs.* SHE) (See Table 1 and references therein). The cathodic limit for a flat GUITAR electrode is −0.9 V (*vs.* SHE) as obtained from the cyclic voltammogram. This is similar to a previous study with GUITAR electrodes [22]. On the graphite felt electrode of this study, the hydrogen wave onset is estimated at −0.4 V (*vs.* SHE) at 200 μA/cm^2 and lies within the range of literature graphitic materials. It is important to note that the cathodic limit of the felt electrodes, both bare and GUITAR-coated is calculated based on the true surface area. On the GUITAR-coated graphite felt electrode, the hydrogen wave onset potential is −0.75 V (*vs.* SHE), a 350 mV increase in overpotential relative to the bare felt.

Table 1. Cathodic potential limits (*vs.* SHE) at 200 μA/cm^2 for various carbon materials in 1M H_2SO_4 as measure by cyclic voltammetry at 50 mV/s. The number of runs (n) and the standard deviations are also reported.

Material	Cathodic Limit (V) *vs.* SHE	Reference
GUITAR	−0.90 ± 0.07 (n = 5)	This work
GUITAR/KFD graphite felt	−0.75 ± 0.05 (n = 5)	This work
Pyrolytic Graphite	−0.52 ± 0.06	[22]
KFD Graphite felt	−0.40 ± 0.05 (n = 5)	This work
Graphite *	−0.4 to −0.5	[3–5]
Glassy carbon	−0.3 to −0.5	[3–5]

* Graphite includes highly ordered pyrolytic graphite (HOPG) and exfoliated graphite.

2.3. Estimation of $V^{3+/2+}$ HET Rates by Cyclic Voltammetry (CV)

The HET rates of $V^{3+/2+}$ redox couple is relatively slow on most graphitic materials (see Table 2). The sequence of CV curves for the $V^{3+/2+}$ (0.050 M VCl_3, 1 M H_2SO_4) redox couple on flat GUITAR flake, bare KFD graphite felt, and GUITAR-coated graphite felt electrodes are shown in Figure 3A–C, respectively. Scan rate variation on KFD graphite felt and GUITAR/KFD felt electrode in 1 mM $Fe(CN)_6^{3-/4-}$ (in 1 M KCl) showed semi-infinite diffusion behavior (where peak current is proportional to the square root of scan rate) at and above 75 mV/s (Figures S1 and S2). Cyclic voltammograms were recorded at a scan rate of 200 mV/s to avoid the thin layer voltammetry (where peak current is directly proportional to the scan rate) [37]. The cathodic peak current density is 25 ± 2 mA/cm^2 (n = 3) on the flat GUITAR electrode (Figure 3A) at −1.2 V (*vs.* Ag/AgCl). The peak current density is measured based on geometric area of the electrode. This corresponds to a standard rate constant (k^0) of 4.8 × 10^{-6} cm/s when modelled through Digisim software. For the bare KFD felt electrode, the cathodic peak current density is 150 ± 10 mA/cm^2 (n = 3) (Figure 3B) at −1.2 V (*vs.* Ag/AgCl) which corresponds to a modelled standard rate constant (k^0) of 8.2 × 10^{-7} cm/s. For the GUITAR-coated KFD felt electrode, the cathodic peak current density is 420 ± 20 mA/cm^2 (n = 3) at −1.2 V (*vs.* Ag/AgCl) which corresponds to a modelled standard rate constant (k^0) of 8.6 × 10^{-6} cm/s that is 10 times faster than the k^0 for the bare KFD graphite felt system (Figure 3C). This is despite the apparent decrease in true surface area with GUITAR-coated KFD electrodes (61.6 cm^2/cm^2 geometric area). HET rates are much faster than the bare KFD graphite felt systems (64.4 cm^2/cm^2 geometric area). The GUITAR-coated KFD electrode exhibits significantly higher current density over the bare KFD felt (Figure 3B,C). This improvement in HET rates with GUITAR/KFD electrodes was discussed in a previous publication [22].

Graphitic materials have a well-known anisotropy in HET rates between the basal and edge planes. In general, the edge plane (EP) is much faster at these rates by several orders of magnitude over the basal plane (BP) [38,39]. This is very acute in crystalline graphites where the density of electronic states near the Fermi level is very low [38]. Also noteworthy is that the majority of exposed graphitic surface of KFD fibers is expected to be basal plane in nature. In previous investigations,

the BP-GUITAR was found to have HET rates for $Fe(CN)_6^{4-/3-}$ similar to those of its EP-GUITAR and EP-graphites. The k^0 rates for BP-GUITAR (10^{-2} cm/s) surpasses those for BP-highly oriented pyrolytic graphite (HOPG) and BP-graphene by five or more orders of magnitude [1,22]. The $V^{3+/2+}$ redox couple does not exhibit enhanced HET kinetics on the BP-GUITAR as opposed to literature BP-HOPG (Table 2), with both being about 10^{-6} cm/s. McCreery classifies the $V^{3+/2+}$ as a redox species whose HET rates are catalyzed by surface oxides [40]. Elemental analysis of GUITAR by XPS reveals that it has a low surface oxygen content [30]. Modification of the GUITAR surface with oxide groups for improved HET rates will be a focus of future investigations.

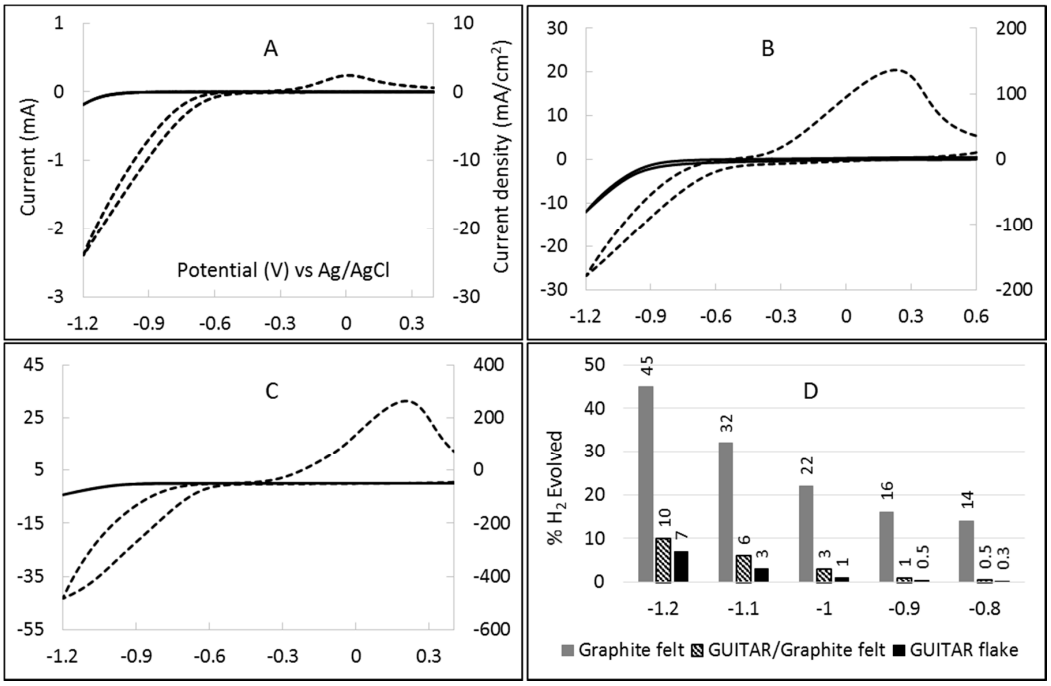

Figure 3. Cyclic voltammograms of background (in 1 M H_2SO_4, solid line) and $V^{3+/2+}$ (0.05 M in 1 M H_2SO_4 dashed lines) obtained at the (**A**) flat GUITAR electrode (0.10 cm^2), (**B**) KFD graphite felt electrode (geometric area 0.16 cm^2), and (**C**) GUITAR/KFD graphite felt electrode (geometric area 0.10 cm^2). All cyclic voltammograms were obtained at a scan rate of 200 mV/s. The percentage H_2 evolutions on different electrodes at different potentials (V) are shown in (**D**).

2.4. Percentage Hydrogen Evolution

Figure 3D shows hydrogen production as a percentage of total current. The percent of hydrogen evolution was calculated as the ratio of background current (in 1 M H_2SO_4) to V^{3+} reduction current (0.05 M V^{3+} in 1 M H_2SO_4) at a scan rate of 200 mV/s on three electrodes. These are estimated from the cyclic voltammetric waves in Figure 3. At −1.0 V, the percentage of hydrogen evolution on flat GUITAR and GUITAR/KFD graphite felt electrodes are observed as 1% and 3%, respectively. On bare KFD graphite felt, 22% of the total current is attributable to hydrogen production (Figure 3D and Table 3). When compared to literature, GUITAR flake and GUITAR-coated KFD graphite felt electrodes are the lowest reported for the fraction of the total cathodic current diverted to hydrogen evolution. This high overpotential for hydrogen evolution is not well understood and was reported in a previous publication [22]. The hydrophobicity of GUITAR may diminish proton adsorption on its surface. The detailed mechanism of this behavior, however, is not well understood and is a subject of future study. Table 3 highlights the relevant literature. The fraction (as percent) of the total current that evolves hydrogen ranges from a few % to greater than 50%. These values are stated within the publication or calculated from the data in the respective figure mentioned in the table. No other materials approach GUITAR's performance of 1% hydrogen current at −1.0 V (*vs.* Ag/AgCl) in 1 M H_2SO_4.

Table 2. Comparison of standard heterogeneous electron transfer rate constants for $V^{3+/2+}$ redox at various carbon materials. See Figure 3 for corresponding cyclic voltammograms.

Material	Geometric Surface Area (cm^2)	True Surface Area (cm^2)	HET Rate Constant (k^0) for $V^{3+/2+}$ (cm/s)	Reference
GUITAR/KFD graphite felt	0.10	6.1	8.6×10^{-6}	This work
GUITAR flake	0.10	0.10	4.8×10^{-6}	This work
KFD graphite felt	0.16	10.3	8.2×10^{-7}	This work
Non-porous flat electrodes				
Edge plane pyrolytic graphite			3.5×10^{-5}–5.5×10^{-4}	[21,41]
Glassy carbon	0.07		1.7×10^{-5}–5.4×10^{-5}	[21,41]
Basal plane highly ordered pyrolytic graphite	0.02		$<3.0 \times 10^{-6}$	[42]
High surface area electrodes				
Graphite reinforcement carbon	0.08		4.8×10^{-3}–9.7×10^{-3}	[26]
Plastic formed carbon			5.3×10^{-4}	[41]
Carbon felt	3.0		1.5×10^{-7}	[14]
Carbon paper	0.13	128	1.07×10^{-3}–3.28×10^{-3}	[21]

Table 3. Comparison of H_2 evolution as a percentage of total current at different carbon electrodes. See Figure 3 for the corresponding cyclic voltammograms. The specific potentials and V^{3+} and H_2SO_4 concentrations are noted.

Material	% H_2	Potential (V)	Conditions	How Calculated? and Ref.
GUITAR flake	1	−1.0 *vs.* Ag/AgCl	0.05 M V^{3+} 1 M H_2SO_4	Figure 3 This work
	0.3	−0.8 *vs.* Ag/AgCl		
GUITAR coated KFD graphite felt	3	−1.0 *vs.* Ag/AgCl		
	0.5	−0.8 *vs.* Ag/AgCl		
KFD graphite felt	22	−1.0 *vs.* Ag/AgCl		
	14	−0.8 *vs.* Ag/AgCl		
Graphite	78	−1.0 *vs.* SCE	0.1 M V^{3+} 2 M H_2SO_4	Stated Figure 2b in ref. [17]
	22	−0.8 *vs.* SCE		
Graphite	20	−0.65 *vs.* SCE	1 M V^{3+} 5 M H_2SO_4	Calculated Figure 1a,b in ref. [43]
Graphite felt	5–8	−0.65 *vs.* Ag/AgCl	0.05 M V^{3+} 1 M H_2SO_4	Calculated Figures 2b, 4 in ref. [19]
Carbon felt	20		2 M V^{3+} 2.5 M H_2SO_4	Stated Figure 6b in ref. [44]
Glassy carbon	80	−1.0 *vs.* SCE	0.08 M V^{3+} 1.8 M H_2SO_4	Calculated Figure 2 in ref. [45]
Porous carbon paper	10–22		1 M V^{3+} H_2SO_4:HNO_3=3:1	Stated Table 5 in ref. [46]
Carbon nanotubes	15	−0.65 *vs.* SCE	1 M V^{3+} 5 M H_2SO_4	Calculated Figure 1a,b in ref. [44]
WO_3/ASC/CP *	5–9		0.05 M V^{3+} 3 M H_2SO_4	Stated Table 3 in ref. [47]
Titanium nitride/Carbon paper	12	−0.7 *vs.* SCE	0.1 M V^{3+}, 1 M H_2SO_4	Calculated Figure 2 in ref. [33]
Graphite plate	10	−0.75 *vs.* SCE	1.6 M V^{3+} 3 M H_2SO_4	Calculated Figures 3,6 in ref. [32]

* Carbon paper coated with super activated carbon supported tungsten trioxide.

3. Materials and Methods

Materials and chemicals: Graphite felt (KFD 2.5 EA type, with a thickness of 2.5 mm) was donated by SGL Carbon Company (St. Marys, PA, USA). Sulfuric acid (96.3%) was obtained from the J.T Baker Chemical Co. (Phillipsburg, NJ, USA). Vanadium (III) chloride (97%) was obtained from Sigma-Aldrich (St. Louis, MO, USA). Ethyl alcohol (99.5%) was obtained from Pharmco Products Inc. (Brookfield, CT, USA). Potassium chloride was obtained from Fisher Scientific (Waltham, NJ, USA) and potassium ferricyanide was obtained from Acros Organics (Morris Plains, NJ, USA). Black-Jack All Weather Roof Cement (Gardner-Gibson, Inc. Tampa, FL, USA) was used as GUITAR precursor. A quartz tube was obtained from Technical Glass Products, Inc. (Painesville Twp., OH, USA), cut into small wafers (approximately 20 mm × 6 mm), and used as GUITAR deposition substrate. Copper alligator clips (model: CTM-34C) were obtained from Cal Test Electronics (Yorba Linda, CA, USA). Paraffin wax (Gulf wax) was obtained from Royal Oak Enterprises (Roswell, GA, USA). All aqueous solutions were prepared with deionized water which was purified by passage through an activated carbon purification cartridge (Barnstead, model D8922, Dubuque, IA, USA).

Electrode fabrication and electrochemical cell setup: GUITAR was synthesized as described by previous procedures through the thermolyzed asphalt reaction (TAR) [2,30,48]. Deposition of GUITAR onto graphite felt was achieved by this method [30,48]. Graphite felt strips were placed into the crucible prior to the TAR method which allowed GUITAR deposition on the felt fibers. An aliquot of 30 g of roofing tar was used to coat a single batch of graphite felt (3 pieces, each of 15 mm × 5 mm). The coating process took 30–35 min. Both the KFD felt and GUITAR/KFD felt electrodes were encased with paraffin wax in order to obtain a specific geometric area. Ohmic contact was made with a copper alligator clip (Figure S2). Electrodes were then made hydrophilic prior to any voltammetric measurements. This was achieved by washing in ethanol, rinsing with deionized water, followed by agitation in the electrochemical cell solution as proposed by Smith *et al.* [35].

All electrochemical studies were conducted in a three-electrode undivided cell with a reticulated vitreous carbon basket counter electrodes (Bioanalytical Systems, Inc. West Lafayette, IN, USA) and an Ag/AgCl/3M NaCl (aq) (0.209 V *vs.* SHE) reference electrode. Cyclic voltammetry (CV) was carried out using a Bioanalytical Systems CV-50W potentiostat (West Lafayette, IN, USA). The supporting electrolytes (1 M H_2SO_4) were de-aerated by bubbling with N_2 (g) for 15 min before addition of VCl_3. All the solutions were de-aerated by purging with N_2 (g) for at least 15 min before recording cyclic voltammograms.

Modelling of Cyclic Voltammetric Curves: The standard rate constants (k^0, cm/s) were determined by modeling experimental voltammograms with Digisim version 3.03b software (Bioanalytical Systems, Inc. West Lafayette, IN, USA). All CVs were corrected for background hydrogen waves. The transfer coefficient (α) is assumed as 0.5 as used in modelling of $V^{3+/2+}$ HET rates in literature [21,49]. The modeling software converged on a diffusion coefficient of 6×10^{-6} cm^2/s which is also within the range reported in literatures (1.4×10^{-6} to 8.4×10^{-6} cm^2/s) [21,45,49]. Semi-infinite linear diffusion system was considered during the simulation. The half wave potential ($E_{1/2}$ = ½ (E_{pc} + E_{pa})) was calculated as −0.490 V. Scan rate and concentrations (for V^{3+}) used were 0.2 V/s and 0.05 M, respectively. The uncompensated solution resistances were considered as 1.0 Ω for both the KFD felt and the GUITAR/KFD felt and 15.0 Ω for GUITAR flake during the simulation and were measured using the potentiostat.

4. Conclusions

This investigation indicates that the application of GUITAR coatings to existing carbon materials for the negative electrode of the VRFB is a viable method for the reduction of parasitic hydrogen gassing as well as increasing the slow HET rates for $V^{3+/2+}$. The HET rate for $V^{3+/2+}$ (0.05 M V^{3+} in 1.0 M H_2SO_4) on GUITAR-coated KFD felt is 10 times faster than that of the bare KFD graphite felt with a total current that contributes only 3% hydrogen evolution at −1.0 V (*vs.* Ag/AgCl). Future endeavors will examine the mechanism for V^{3+} reduction, the observed decrement of hydrogen evolution at the negative

electrode, as well as the positive ($V^{5+/4+}$) electrode reactions on GUITAR surface. It is expected that GUITAR will enhance the positive electrode performance from the standpoint of corrosion resistance.

Supplementary Materials: Supplementary materials can be found at http://www.mdpi.com/2311-5629/2/2/13/s1.

Acknowledgments: The authors acknowledge the University of Idaho for its support of the graduate students through teaching assistantships and to SGL Carbon Company (St. Marys, PA, USA) for the donation of the KFD graphite felt.

Author Contributions: A major portion of the experimental works including electrode preparation, $V^{2+/3+}$ study and cathodic limit measurement on flat GUITAR, KFD graphite felt and GUITAR/KFD felt were done by Humayun Kabir. Haoyu Zhu helped to acquire the scanning electron micrographs. The Digisim modelling to calculate the HET rate constants were jointly done by Humayun Kabir and Isaiah O. Gyan. Jeremy D. Foutch helped to prepare the manuscript. Finally, this project is designed, coordinated and supervised by I. Francis Cheng.

Conflicts of Interest: The authors declare no conflict of interest.

Abbreviations

The following abbreviations are used in this manuscript:

GUITAR	Graphene from the University of Idaho Thermolyzed Asphalt Reaction
HET	Heterogeneous electron transfer
DOS	Density of electronic states
RFB	Redox flow batteries
VRFB	Vanadium redox flow battery
SHE	Standard hydrogen electrode
SCE	Saturated calomel electrode
EP	Edge plane
BP	Basal plane

References

1. Gyan, I.O.; Cheng, I.F. Electrochemical study of biologically relevant molecules at electrodes constructed from GUITAR, a new carbon allotrope. *Microchem. J.* **2015**, *122*, 39–44. [CrossRef]
2. Cheng, I.F.; Xie, Y.; Gyan, I.O.; Nicholasa, N.W. Highest measured anodic stability in aqueous solutions: Graphenic electrodes from the thermolyzed asphalt reaction. *RSC Adv.* **2013**, *3*, 2379–2384. [CrossRef]
3. Tanaka, Y.; Furuta, M.; Kuriyama, K.; Kuwabara, R.; Katsuki, Y.; Kondo, T.; Fujishima, A.; Honda, K. Electrochemical properties of N-doped hydrogenated amorphous carbon films fabricated by plasma-enhanced chemical vapor deposition methods. *Electrochim. Acta* **2011**, *56*, 1172–1181. [CrossRef]
4. Martin, H.B.; Argoitia, A.; Landau, U.; Anderson, A.B.; Angus, J.C. Hydrogen and Oxygen Evolution on Boron-Doped Diamond Electrodes. *J. Electrochem. Soc.* **1996**, *143*, L133–L136. [CrossRef]
5. Ndlovu, T.; Sampath, O.A.A.S.; Krause, R.W.; Mamba, B.B. Reactivities of Modified and Unmodified Exfoliated Graphite Electrodes in Selected Redox Systems. *Int. J. Electrochem. Sci.* **2012**, *7*, 9441–9453.
6. Li, L.; Kim, S.; Wang, W.; Vijayakumar, M.; Nie, Z.; Chen, B.; Zhang, J.; Xia, G.; Hu, J.; Graff, G.; *et al.* A Stable Vanadium Redox-Flow Battery with High Energy Density for Large-Scale Energy Storage. *Adv. Energy Mater.* **2011**, *1*, 394–400. [CrossRef]
7. Li, W.; Liu, J.; Yan, C. Graphite-graphite oxide composite electrode for vanadium redox flow battery. *Electrochim. Acta* **2011**, *56*, 5290–5294. [CrossRef]
8. Joerissen, L.; Garche, J.; Fabjan, C.; Tomazic, G. Possible use of vanadium redox-flow batteries for energy storage in small grids and stand-alone photovoltaic systems. *J. Power Sources* **2004**, *127*, 98–104. [CrossRef]
9. Fetyan, A.; Derr, I.; Kayarkatte, M.K.; Langner, J.; Bernsmeier, D.; Kraehnert, R.; Roth, C. Electrospun Carbon Nanofibers as Alternative Electrode Materials for Vanadium Redox Flow Batteries. *ChemElectroChem* **2015**. [CrossRef]

10. Xi, J.; Wu, Z.; Teng, X.; Zhao, Y.; Chen, L.; Qiu, X. Self-assembled polyelectrolyte multilayer modified Nafion membrane with suppressed vanadium ion crossover for vanadium redox flow batteries. *J. Mater. Chem.* **2008**, *18*, 1232–1238. [CrossRef]
11. Kear, G.; Shah, A.A.; Walsh, F.C. Development of the all-vanadium redox flow battery for energy storage: A review of technological, financial and policy aspects. *Int. J. Energy Res.* **2012**, *36*, 1105–1120. [CrossRef]
12. Weber, A.Z.; Mench, M.M.; Meyers, J.P.; Ross, P.N.; Gostick, J.T.; Liu, Q.H. Redox flow batteries: A review. *J. Appl. Electrochem.* **2011**, *41*, 1137–1164. [CrossRef]
13. Yang, Z.; Zhang, J.L.; Kintner-Meyer, M.C.W.; Lu, X.; Choi, D.; Lemmon, J.P.; Liu, J. Electrochemical Energy Storage for Green Grid. *Chem. Rev.* **2011**, *111*, 3577–3613. [CrossRef] [PubMed]
14. Agar, E.; Dennison, C.R.; Knehr, K.W.; Kumbur, E.C. Identification of performance limiting electrode using asymmetric cell configuration in vanadium redox flow batteries. *J. Power Sources* **2013**, *225*, 89–94. [CrossRef]
15. Aaron, D.; Sun, C.; Bright, M.; Papandrew, A.B.; Mench, M.M.; Zawodzinski, T.A. *In Situ* Kinetics Studies in All-Vanadium Redox Flow Batteries. *ECS Electrochem. Lett.* **2013**, *2*, A1–A3. [CrossRef]
16. Agar, E.; Dennison, C.R.; Knehr, K.W.; Kumbur, E.C. Asymmetric performance testing of carbon felt electrodes to identify the limiting electrode in vanadium redox flow batteries. *ECS Trans.* **2013**, *53*, 69–73. [CrossRef]
17. Chen, F.; L, J.; Chen, H.; Yan, C. Study on Hydrogen Evolution Reaction at a Graphite Electrode in the All-Vanadium Redox Flow Battery. *Int. J. Electrochem. Sci.* **2012**, *7*, 3750–3764.
18. Sun, C.; Delnick, F.M.; Baggetto, L.; Veith, G.M.; Zawodzinski, T.A. Hydrogen evolution at the negative electrode of the all-vanadium redox flow batteries. *J. Power Sources* **2014**, *248*, 560–564. [CrossRef]
19. Surez, D.J.; Gonzlez, Z.; Blanco, C.; Granda, M.; Menndez, R.; Santamara, R. Graphite Felt Modified with Bismuth Nanoparticles as Negative Electrode in a Vanadium Redox Flow Battery. *ChemSusChem* **2014**, *7*, 914–918. [CrossRef] [PubMed]
20. Parasuraman, A.; Lim, T.M.; Menictas, C.; Skyllas-Kazacos, M. Review of material research and development for vanadium redox flow battery applications. *Electrochim. Acta* **2013**, *101*, 27–40. [CrossRef]
21. Wu, X.W.; Tomoo, Y.; Suguru, O.; Zhang, Q.X.; Lv, F.C.; Liu, C.M.; Shirasaki, K.; Satoh, I.; Shikama, T.; Lu, D. Acceleration of the redox kinetics of VO^{2+}/VO_2^{+} and V^{3+}/V^{2+} couples on carbon paper. *J. Appl. Electrochem.* **2011**, *41*, 1183–1190. [CrossRef]
22. Gyan, I.O.; Wojcik, P.M.; Aston, D.E.; McIlroy, D.N.; Cheng, I.F. A Study of the Electrochemical Properties of a New Graphitic Material: GUITAR. *ChemElectroChem* **2015**, *2*, 700–706. [CrossRef]
23. Li, X.; Zhang, H.; Mai, Z.; Zhang, H.; Vankelecom, I. Ion exchange membranes for vanadium redox flow battery (VRB) applications. *Energy Environ. Sci.* **2011**, *4*, 1147–1160. [CrossRef]
24. Huang, K.-L.; Li, X.-G.; Liu, S.-Q.; Tan, N.; Chen, L.-Q. Research progress of vanadium redox flow battery for energy storage in China. *Renew. Energy* **2008**, *33*, 186–192. [CrossRef]
25. Zhong, S.; Kazacos, P.M.; Skyllas-Kazacos, M. Comparison of the physical, chemical and electrochemical properties of rayon and polyacrylonitrile-based graphite felt electrodes. *J. Power Sources* **1993**, *45*, 29–41. [CrossRef]
26. Kaneko, H.; Nozaki, K.; Wada, Y.; Aoki, T.; Negishi, A.; Kamimoto, M. Vanadium redox reactions and carbon electrodes for vanadium redox flow battery. *Electrochim. Acta* **1991**, *36*, 1191–1196. [CrossRef]
27. Sun, B.; Skyllas-Kazakos, M. Chemical modification and electrochemical behaviour of graphite fibre in acidic vanadium solution. *Electrochim. Acta* **1991**, *36*, 513–517. [CrossRef]
28. Lee, H.; Kim, H. Development of nitrogen-doped carbons using the hydrothermal method as electrode materials for vanadium redox flow batteries. *J. Appl. Electrochem.* **2013**, *43*, 553–557. [CrossRef]
29. Han, P.; Yue, Y.; Liu, Z.; Xu, W.; Zhang, L.; Xu, H.; Dong, S.; Cui, G. Graphene oxide nanosheets/multi-walled carbon nanotubes hybrid as an excellent electrocatalytic material towards VO^{2+}/VO^{2+} redox couples for vanadium redox flow batteries. *Energy Environ. Sci.* **2011**, *4*, 4710–4717. [CrossRef]
30. Cheng, I.F.; Xie, Y.; Gonzales, R.A.; Gonzales, P.R.; Sundararajan, J.P.; Fouetio Kengne, B.A.; Aston, D.E.; McIlroy, D.N.; Foutch, J.D.; Griffiths, P.R. Synthesis of graphene paper from pyrolyzed asphalt. *Carbon* **2011**, *49*, 2852–2861. [CrossRef]
31. Ding, C.; Zhang, H.; Li, X.; Liu, T.; Xing, F. Vanadium Flow Battery for Energy Storage: Prospects and Challenges. *J. Phys. Chem. Lett.* **2013**, *4*, 1281–1294. [CrossRef] [PubMed]
32. Shen, J.; Liu, S.; He, Z.; Shi, L. Influence of antimony ions in negative electrolyte on the electrochemical performance of vanadium redox flow batteries. *Electrochim. Acta* **2015**, *151*, 297–305. [CrossRef]

33. Yang, C.; Wang, H.; Lu, S.; Wu, C.; Liu, Y.; Tan, Q.; Liang, D.; Xiang, Y. Titanium nitride as an electrocatalyst for V(II)/V(III) redox couples in all-vanadium redox flow batteries. *Electrochim. Acta* **2015**, *182*, 834–840. [CrossRef]
34. Huang, X. Fabrication and Properties of Carbon Fibers. *Materials* **2009**, *2*, 2369–2403. [CrossRef]
35. Smith, R.E.G.; Davies, T.J.; Baynes, N.B.; Nichols, R.J. The electrochemical characterisation of graphite felts. *J. Electroanal. Chem.* **2015**, *747*, 29–38. [CrossRef]
36. Flox, C.; Rubio-Garcia, J.; Nafria, R.; Zamani, R.; Skoumal, M.; Andreu, T.; Arbiol, J.; Cabot, A.; Morante, J.R. Active nano-$CuPt_3$ electrocatalyst supported on graphene for enhancing reactions at the cathode in all-vanadium redox flow batteries. *Carbon* **2012**, *50*, 2347–2374. [CrossRef]
37. Bard, A.J.; Faulkner, L.R. *Electrochemical Methods: Fundamentals and Applications*, 2nd ed.; Wiley: New York, NY, USA, 2000; p. 455.
38. Rice, R.J.; McCreery, R.L. Quantitative Relationship between Electron Transfer Rate and Surface Microstructure of Laser-Modified Graphite Electrodes. *Anal. Chem.* **1989**, *61*, 1637–1641. [CrossRef]
39. Pour, N.; Kwabi, D.G.; Carney, T.; Darling, R.M.; Perry, M.L.; Shao-Horn, Y. Influence of Edge- and Basal-Plane Sites on the Vanadium Redox Kinetics for Flow Batteries. *J. Phys. Chem. C* **2015**, *119*, 5311–5318. [CrossRef]
40. Smith, R.E.G.; Davies, T.J.; de B. Baynes, N.; Nichols, R.J. The electrochemical characterisation of graphite felts. *J. Electroanal. Chem.* **2015**, *747*, 29–38. [CrossRef]
41. McCreery, R.L. Advanced Carbon Electrode Materials for Molecular Electrochemistry. *Chem. Rev.* **2008**, *108*, 2646–2687. [CrossRef] [PubMed]
42. Yamamura, T.; Watanabe, N.; Yano, T.; Shiokawa, Y. Electron-Transfer Kinetics of Np^{3+}/Np^{4+}, NpO_2^{+}/NpO_2^{2+}, V^{2+}/V^{3+}, and VO^{2+}/VO_2^{+} at Carbon Electrodes. *J. Electrochem. Soc.* **2005**, *152*, A830–A836. [CrossRef]
43. McDermott, C.A.; Kneten, K.R.; McCreery, R.L. Electron Transfer Kinetics of Aquated $Fe^{+3/+2}$, $Eu^{+3/+2}$, and $V^{+3/+2}$ at Carbon Electrodes: Inner Sphere Catalysis by Surface Oxides. *J. Electrochem. Soc.* **1993**, *140*, 2593–2599. [CrossRef]
44. Zhu, H.Q.; Zhang, Y.M.; Yue, L.; Li, W.S.; Li, G.L.; Shu, D.; Chen, H.Y. Graphite-carbon nanotube composite electrodes for all vanadium redox flow battery. *J. Power Sources* **2008**, *184*, 637–640. [CrossRef]
45. Kim, K.J.; Kim, Y.-J.; Kim, J.-H.; Park, M.-S. The effects of surface modification on carbon felt electrodes for use in vanadium redox flow batteries. *Mater. Chem. Phys.* **2011**, *131*, 547–553. [CrossRef]
46. Sum, E.; Skyllas-kazacos, M. A study of the V(II)/V(III) redox couple for redox flow cell applications. *J. Power Sources* **1985**, *15*, 179–190. [CrossRef]
47. Yue, L.; Li, W.; Sun, F.; Zhao, L.; Xing, L. Highly hydroxylated carbon fibers as electrode materials of all-vanadium redox flow battery. *Carbon* **2010**, *48*, 3079–3090. [CrossRef]
48. Yao, C.; Zhang, H.; Liu, T.; Li, X.; Liu, Z. Carbon paper coated with supported tungsten trioxide as novel electrode for all-vanadium flow battery. *J. Power Sources* **2012**, *218*, 455–461. [CrossRef]
49. Xie, Y.; McAllister, S.D.; Hyde, S.A.; Sundararajan, J.P.; FouetioKengne, B.A.; McIlroy, D.N.; Cheng, I.F. Sulfur as an important co-factor in the formation of multilayer graphene in the thermolyzed asphalt reaction. *J. Mater. Chem.* **2012**, *22*, 5723–5729. [CrossRef]